7

Doped Fiber Amplifier Characteristic Under Internal and External Perturbation

Siamak Emami[1], Hairul Azhar Abdul Rashid[2],
Seyed Edris Mirnia[1], Arman Zarei[1],
Sulaiman Wadi Harun[1] and Harith Ahmad[1]
[1]*University of Malaya Malaysia,*
[2]*Multimedia University Malaysia,*
Malaysia

1. Introduction

Significant effort has been made in recent years to improve the Doped Fiber amplifier gain and noise figure. Extend the optical bandwidth of doped fiber amplifiers beyond the traditional 1550nm band, making the excellent EDFA characteristics available in a wider spectral region also was the main effort in optical amplifier fields. Several techniques have been developed to improve gain and shift the gain to the shorter wavelength region. In this chapter, the effects of external perturbation such as macro-bending and fiber length and internal perturbation such as transversal distribution profile and doped concentration on doped fiber performance have been demonstrated (S.D.Emami et al., 2010).

A macro-bending approach is demonstrated to increase a gain and noise figure at a shorter wavelength region of EDFA. The conventional double-pass configuration is used for the EDFA to obtain a higher gain with a shorter length and lower pump power. The macro-bending suppresses the ASE at longer wavelength to achieve a higher population inversion at shorter wavelengths. Without the bending, the peak ASE at 1530nm, which is a few times higher than the ASE at the shorter wavelength, would deplete the population inversion and suppresses the gain in this region.

Macro-bending is introduced as a new method to increase gain flatness and bandwidth of EDFA in C-band region. Varying the bending radius and doped fiber length leads to the optimized condition with flatter and broader gain profile. Under the optimized condition, gain at shorter wavelengths is increased due to increment of population inversion which results in gain reduction in the longer wavelength regions. The balance of these two effects in the optimized condition has a significant result in achieving a flattened and broadened gain profile.

This technique is also capable to compensate the fluctuation in operating temperatures due to proportional temperature sensitivity of absorption cross section and bending loss of the aluminosilicate EDF . This new approach can be used to design a temperature insensitive EDFA for application in a real optical communication system which operates at different environments but still maintaining the gain characteristic regardless of temperature variations. The effect of macro-bending on high concentration EDFA using optimized

bending radius and length of the doped fiber is demonstrated. This gain increment compensates the gain reduction of the EDF before applying macro-bending and result in a flat and broad gain spectrum.
One of the many EDFA optimization parameters reported includes the Erbium Transversal Distribution Profile (TDP). The Erbium TDP is essential in determining the overlap factor, which affects the absorption and emission dynamics of the EDFA. At the end of this chapter, numerical models of different Erbium TDP is demonstrated and later verified by experiment. The model considers the overlap factor and absorption/ emission dynamics for different Erbium TDP. Results indicate a high performance EDFA is achievable with an optimized and yet realistic Erbium TDP.

2. Macrobending effects on doped fiber amplifier

In the first part of this chapter, a macrobending approach is demonstrated to increase the gain and noise figure at a shorter wavelength region of EDFA. The conventional double pass configuration is used for the EDFA to obtain a higher gain with a shorter length and lower pump power. The macrobending suppresses the ASE at a longer wavelength to achieve a higher population inversion at shorter wavelengths. Without the bending, the peak ASE at 1530 nm, which is a few times higher than the ASE at the shorter wavelength, would deplete the population inversion and suppresses the gain in this region (Harun et al., 2008).
The configuration of the EDFA is based on a standard double-pass configuration, where a circulator was used at the input and output ends of the EDF to couple light out of the amplifier and to allow the double propagation of light in the gain medium, respectively. The EDF is pumped by a 980-nm laser diode using a propagating pump scheme. The commercial EDF used is 15 m long with an erbium ion concentration of 440 ppm. A tunable laser source is used to characterize the amplifier in conjunction with an optical spectrum analyzer (OSA). The amplifier is characterized in the wavelength region between 1480 to 1560 nm in terms of the gain and noise figure under changes in the optical power. Before the amplifier experiment, the optical loss of the EDF was characterized for both cases with and without macrobending. The macrobending is obtained by winding the EDF in a bobbin with various radiuses between 0.35 and 0.50 mm (Daud, et al. 2008).
The optical losses of EDF were measured against wavelengths at various radius of macro-bending and the result is compared to the straight EDF. Then the bending loss spectrum (dB/m) is obtained by taking the difference of the optical loss measurement between bent and straight EDF. Fig. 1 shows the bending loss spectrum at various bending radius between 0.35 to 0.50 mm. The experimental result is in agreement with the earlier reported theoretical prediction on bending loss in optical fiber (Thyagarajan & Kakkar, 2004), which uses a simple infinite cladding model. The theoretical result shows that the bending loss profile is almost exponential with respect to wavelength, with strong dependencies on fiber bending radius and refractive index profile. Bending of optical fiber, including EDF causes the propagating power of the guided modes to be transferred into cladding, which in turn resulted in loss of power and therefore the bending loss spectrum is obtained as shown in Fig. 2. The bending loss has a strong spectral variation because of the proportional changes of the mode field diameter with the signal wavelength. At bending radius of 0.40 mm, the experimental result shows that the bending loss is drastically increase (>10 dB/m) at the wavelengths above 1505 nm whereas the minimal loss is observed at the wavelengths below 1505 nm. This provides the ASE suppression of more than 270 dB at 1530 nm, which allows

a higher attainable gain at a shorter wavelength region. This result shows that the distributed ASE filtering can be achieved by macro-bending of the fiber at an optimally chosen radius. This characteristic can be used in research of S-band EDFA and fiber lasers (Daud, et al. 2008).

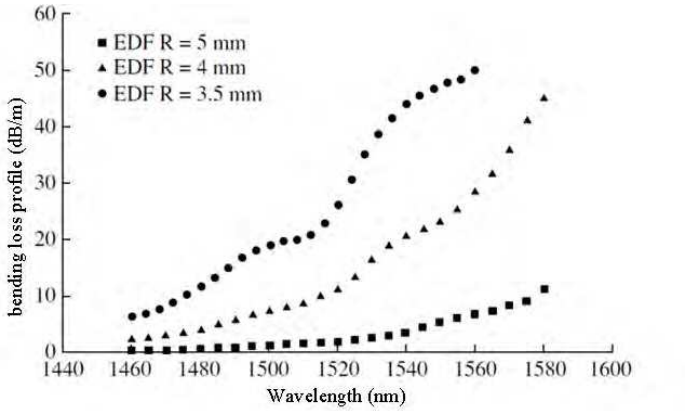

Fig. 1. EDF bending loss profile (dB/m) against wavelength (nm) for different bending radius (3.5 mm, 4 mm and 5 mm).

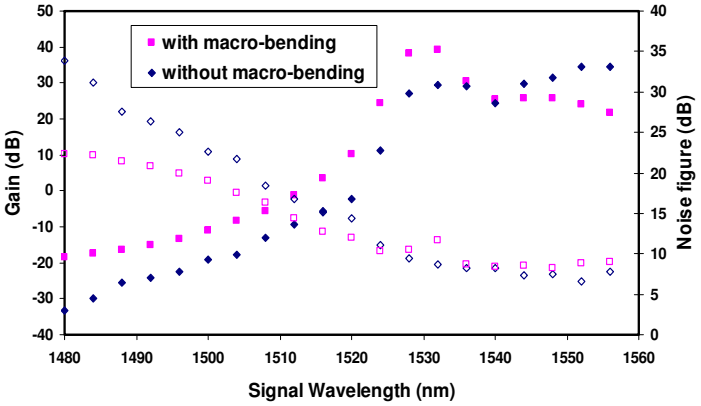

Fig. 2. Gain (solid symbols) and noise figure (hollow symbols) spectra with and without the macro-bending effect. The input signal and pump power is fixed at -30dBm and 100mW, respectively.

Fig. 2 shows the variation of gain and noise figure across the input signal wavelength for the double-pass EDFA with and without the macro-bending. The input signal and 980nm pump powers is fixed at -30 dBm and 100 mW respectively. The bending radius is set at 4 mm in case of the amplifier with the macro-bending. As shown in the figure, the gain enhancements of about 12 ~ 14 dB are obtained with macro-bending at wavelength region between 1480 nm and 1530 nm. This enhancement is attributed to macro-bending effect

which suppresses the ASE at the longer wavelength. This resulted in an increase of population inversion at shorter wavelength, which in turn improves the EDFA's gain at the shorter wavelength as shown in Fig. 2. With the macro-bending, the positive gain is observed for input signal wavelength of 1516 nm and above. On the other hand, the macro-bending also reduces the noise figure of the EDFA at wavelengths shorter than 1525nm as shown in Fig. 2.

Fig. 3 shows the gain and noise figure as a function of 980nm pump power with and without the macro-bending. In this experiment, the input signal power and wavelength is fixed at -30 and 1516nm, respectively. The bending radius is fixed at 4 mm. As shown in the figure, the macro-bending improves both gain and noise figure by approximately 6 dB and 3 dB, respectively. These improvements are due to the longer wavelength ASE suppression by the macro-bending effect in the EDF. With the macro-bending, the double-pass EDFA is able to achieve a positive gain with pump power of 90 mW and above. These results show that the bending effect can be used to increase the gain at a shorter wavelength, which has potential applications in S-band EDFA and fiber lasers. The operating wavelength of EDF fiber laser is expected can be tuned to a shorter wavelength region by the macro-bending.

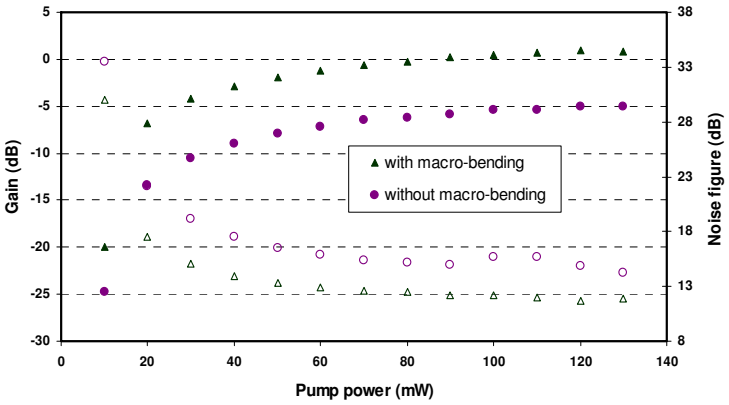

Fig. 3. Gain (solid symbols) and noise figure (hollow symbols) against pump power for EDFAs with and without the macro-bending effect.

3. Application of Macro-Bending Effect on Gain-Flattened EDFA

The configuration of the single pass Macro Bent EDFA used in this research is shown in Fig. 4, which consists of a piece of EDF, a wavelength division multiplexing (WDM) coupler, and a pump laser. An Aluminosilicate host EDF with 1100 ppm erbium ion concentration is used in the setup. Alumina in this fiber is to overcome the quenching effect for high ion concentration. A WDM coupler is used to combine the pump and input signal. Optical isolators are used to ensure unidirectional operation of the optical amplifier. Laser pump power at 980nm is used for providing sufficient pumping power. The EDF is spooled on a rod of 6.5 mm radius to achieve consistent macro-bending effect. The rod has equally spaced threads (8 threads per cm) where each thread houses one turn of EDF to achieve consistency in the desired bending radius. Tunable laser source (TLS) is used to characterize the amplifier in conjunction with the optical spectrum analyzer (OSA) (Hajireza, et al. 2010).

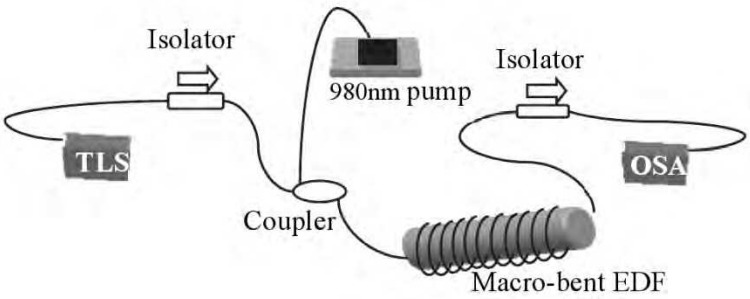

Fig. 4. Configuration of the single-pass EDFA

Initially, the gain and noise figure of the single pass EDFA is characterized without any macro-bending at different EDF lengths. The input signal power is fixed at -30 dBm and the 980 nm pump power is fixed at 200 mW. The wavelength range is chosen between 1520 nm and 1570 nm which covering the entire C-band. It is important to note that using macro-bending to achieve gain flatness depend on suppression of longer wavelength gains. The EDF length used must be slightly longer than the conventional C-band EDFA to allow an energy transfer from C-band to L-band taking place. This will reduce the gain peak at 1530nm and increases the gain at longer wavelengths. The macro-bending provides a higher loss at the longer wavelengths and thus flattening the gain spectrum of the proposed C-band EDFA. The combination of appropriate EDF length and bending radius, leads to flat and broad gain profile across the C-band region.

The bending loss spectrum of the EDF is measured across the wavelength region from 1530 nm to 1570 nm. Fig. 2 illustrates the bending loss profile at bending radius of 4.5 mm, 5.5 mm and 6.5 mm, which clearly show an exponential relationship between the bending loss and wavelength, with strong dependencies on the fiber bending radius. Bending the EDF causes the guided modes to partially couple into the cladding layer, which in turn results in losses as earlier reported. The bending loss has a strong spectral variation because of the proportional changes of the mode field diameter with signal wavelength (Giles et al., 1991) As shown in Fig. 5, the bending loss dramatically increases at wavelengths above 1550 nm. This result shows that the distributed ASE filtering can be achieved by macro bending the EDF at an optimally chosen radius. This provides high ASE or gain suppression around 1560 nm, which reduces the L-band gain. Besides this, lower level suppression of C-band population inversion reduces the effect of gain saturation, providing better C-band gain. Eventually, this characteristic is used to achieve C-band gain flattening in the EDFA (Hajireza, et al. 2010).

The gain spectrum of the EDFA is then investigated when a short length of high concentration EDF spooled in different radius. Fig. 6 shows the gain spectrum of the EDFA with 3m long EDF at different spooling radius. The result was also compared with straight EDF. The input signal power and pump power are fixed at -30dBm and 200 mW respectively in the experiment. As shown in the figure, the original shape of the gain spectrum is maintained in the whole C-band region with the gain decreases exponentially at wavelengths higher than 1560nm. Without bending, the peak gain of 28dB is obtained at 1530 nm which is the reference point to find the optimized length. When the EDF was spooled at a rod with 4.5mm and 5.5mm radius, the shape of gain spectra are totally

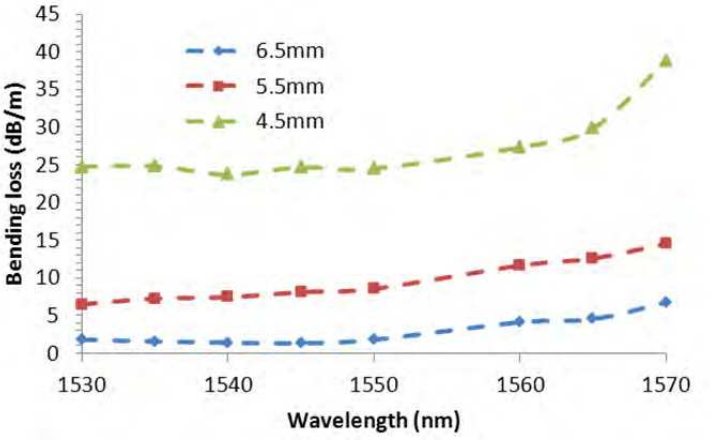

Fig. 5. Bending loss (dB/m) vs. wavelength (nm) for different bending radius

changed. Finally after trying different radius, 6.5 mm was the optimized radius for this amplifier. As shown in Fig. 5, bending loss at radius of 6.5 mm is low especially at wavelengths shorter than 1560nm and therefore the gain spectrum maintains the original shape of the gain spectrum for un-spooled EDF (Hajireza, et al. 2010)..

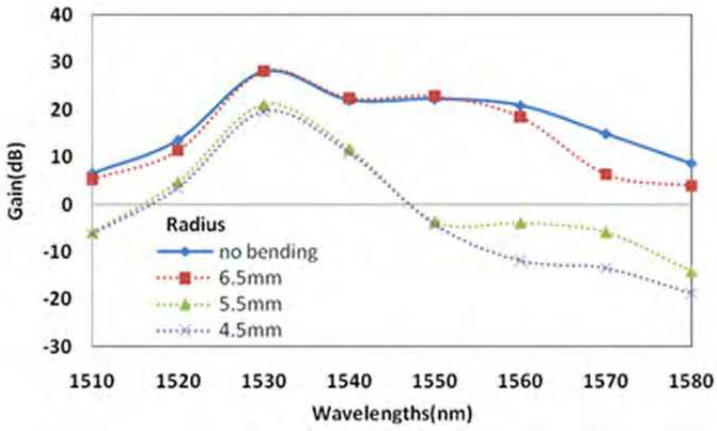

Fig. 6. Efficient length of EDF (3m) in different bending radius for -30dBm input signal]

Fig. 7 shows the gain spectra for the single pass EDFA with unspooled EDF at various EDF lengths. The input signal and 980nm pump powers are fixed at -30 dBm and 200 mW. As the length of the EDF increases, the gain spectrum moves to a longer wavelength region. The C-band photons are absorbed to emit photons at longer wavelength. The overall gain drops at the maximum length of 11m due to the insufficient pump power. Fig. 5 shows the gain spectra for the EDFA with the optimum spooling radius of 6.5 at various EDF lengths.

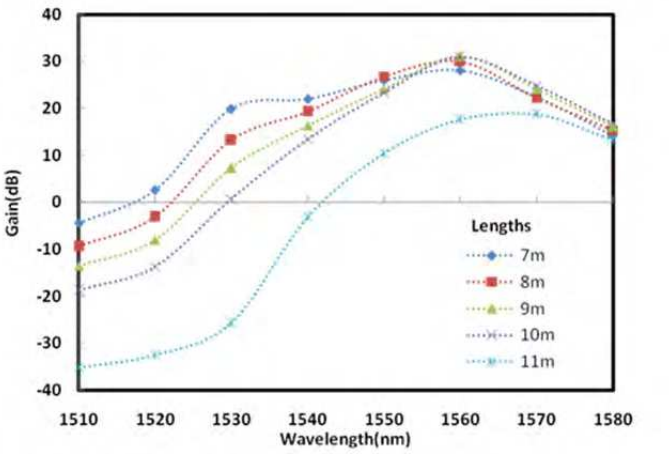

Fig. 7. Gain for un-spooled EDF in different length with -30dBm input signal

To achieve a flatten gain spectrum, the EDFA must operate with insufficient 980nm pump, where the shorter wavelength ASE is absorbed by the un-pumped EDF to emit at the longer wavelength. This will shift the peak gain wavelength from 1530nm to around 1560nm. The macro-bending induces a wavelength dependent bending loss that results in higher loss at longer wavelength compared to the shorter wavelength as shown in Fig. 5. In relation to the EDFA, the macro-bending also suppresses the population inversion in C-band and thus reduces the gain saturation effect in C-band. With this reduced gain saturation, the C-band gain will increase. On the other hand, the L-band gain will reduce due to the suppression of L-band stimulated emission induced by macro-bending. The net effect of both phenomena will result in a flattened gain profile as shown in figure 8. Thus, the level of population inversion is dependent on different parameters such as length of fiber, bending radius and erbium ion concentration of the EDF. The same mechanism of distributed ASE filtering is used for S-band EDFA (Wysocki et al., 1998).

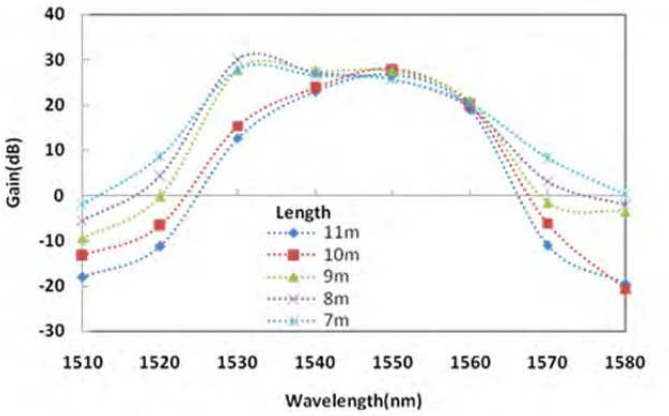

Fig. 8. Gain for 6.5mm spooled radius in different length with -30dBm input signal

Fig. 8 shows a better flattening approach for 9m EDF, where the flattened gain profile is obtained by incremental gain enhancement of about 3 dB and 20 dB at wavelengths of 1550 nm and 1530 nm respectively. This enhancement is attributed to macro-bending effect in the EDF. This incremental gain compensates the incremental gain reduction of the EDFA before applying macro-bending resulting in a flat and broad gain spectrum.

The gain variation to gain ratio ΔG/G is generally used to characterize the gain variation, where ΔG and G are the gain excursion and the average gain value, respectively (Wysocki et al., 1997). In order to define the gain flatness of EDFAs, the ΔG/G for the EDFA with and without macro bending is compared between 1530 and 1555 nm under the same condition. The gain variation ΔG/G for this macro-bent EDFA was 0.10 (2.8 dB / 27.84 dB), which is a 50% improvement compared to earlier reports (Uh-Chan et al., 2002). Besides this, we also observe a gain variation within ±1 dB over 25 nm bandwidth in C-band region (S.D.Emami et al., 2009).

Fig. 9 compares the gain spectrum of the EDFA with and without macro bending EDF at various input signal power. The input signal power is varied for -10 dBm and -30 dBm. The input pump power is fixed at 200 mW. The EDF length and bending radius is fixed at 9m and 6.5 mm respectively. As shown in the figure, increasing the input signal power decreases the gain but improves the gain flatness. The macro bending also reduces the noise figure of EDFA at wavelength shorter than 1550 as shown in Fig. 10 (Hajireza, et al. 2010).

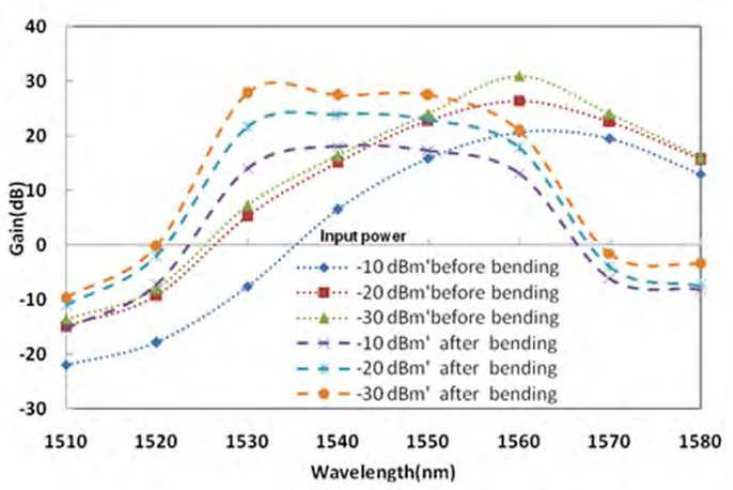

Fig. 9. EDFA gain spectra; with and without acro bending at various input signal power.

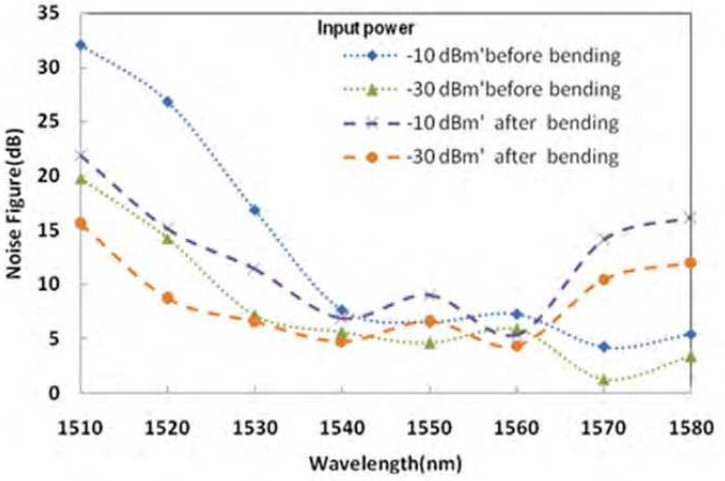

Fig. 10. EDFS noise figure spectra; with and without macro bending at various input signal power.

4. Modelling of the macro-bent EDFA

Macro-bending is defined as a smooth bend of fiber with a bending radius much larger than the fiber radius (Marcuse, 1982). Macro-bending modifies the field distribution in optical fibers and thus changes the spectrum of the wavelength dependent loss. Various mathematical models have been suggested to calculate the bending effects in optical waveguide. Earlier references for bending loss in single mode fibers with step index profiles was developed by Marcuse. According to Marcuse, the total loss of a macro bent fiber includes the pure bending loss and transition loss caused by mismatch between the quasi-mode of the bending fiber and the fundamental mode of the straight fiber (Marcuse, 1976). The analytical expression for a single meter fiber bend loss α can be expressed as follows (Marcuse, 1982):

$$\alpha(\nu) = \frac{\sqrt{\pi}k^2 \exp\left[-\frac{2}{3}\left(\gamma^3 / \beta_g^2\right)R\right]}{e_\nu \gamma^{2/3} V^2 \sqrt{R} K_{\nu-1}(\gamma a) K_{\nu+1}(\gamma a)} \tag{1}$$

where eν=2 , a is the radius of fiber core, R is the bending radius, βg is the propagation constant of the fundamental mode, K(υ-1)(γα) and K(υ+1)(γα) are the modified Bessel functions and V is the well-known normalized frequency, which is defined as (Agrawal, 1997):

$$V = \frac{2\pi a.NA}{\lambda} \tag{2}$$

The values of k and γ can be defined as follows (Gred & Keiser, 2000):

$$k = \sqrt{n_1^2 k^2 - \beta_g^2} \tag{3}$$

$$\gamma = \sqrt{\beta_g^2 - n_2^2 k^2} \tag{4}$$

For an optical fiber with length L, bending loss (α) is obtained by: $\alpha_L = 10\log(\exp(2\alpha l)) = 8.68\alpha L$ Equation (3) agrees well with our experimental results for macro-bent single-mode fiber.

The macro-bent EDFA is modeled by considering the rate equations of a three level energy system. Fig.11 shows the absorption and emission transitions, respectively in the EDFA considering a three-level energy system with 980 nm pump. Level 1 is the ground level, level 2 is the metastable level characterized by a long lifetime, and level 3 the pump level (Armitage, 1988) . The main transition used for amplification is from the 4I13/2 to 4I15/2 energy levels. When the EDF is pumped with 980 nm laser, the ground state ions in the 4I15/2 energy level can be excited to the 4I11/2 energy level and then relaxed to the 4I13/2 energy level by non-radiative decay. The variables N_1, N_2 and N_3 are used to represent population of ions in the $^4I_{15/2}$, $^4I_{13/2}$ and $^4I_{11/2}$ energy levels respectively. According to Fig. 11 we can write the rate of population as follows (Desurvire, 1994):

$$\frac{dN_1}{dz} = -R_{13}N_1 + R_{31}N_3 - W_{12}N_1 + W_{21}N_2 + {}^{R}A_{21}N_2 \tag{5}$$

$$\frac{dN_2}{dt} = -W_{12}N_1 - W_{21}N_2 - {}^{R}A_{21}N_2 + {}^{NR}A_{23}N_3 \tag{6}$$

$$\frac{dN_3}{dz} = R_{13}N_1 - R_{31}N_3 - {}^{NR}A_{32}N_3 \tag{7}$$

$$N_T = N_1 + N_2 + N_3 \tag{8}$$

where R_{13} is the pumping rate from level 1 to level 3 and R_{31} is the stimulated emission rate between level 3 and level 1. The radiative and non radiative decay from level i to s is represented by ${}^{R}A_{ij}$ and ${}^{NR}A_{ij}$. The interaction of the electromagnetic field with the ions or the stimulated absorption and emission rate between level 1 and level 2 is represented by W_{12} and W_{21}.

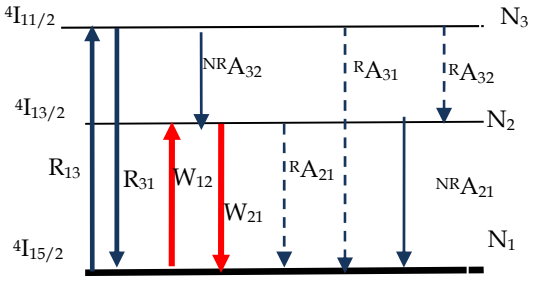

Fig. 11. Three level energy system of EDF pump absorption, and signal transitions.

The stimulated absorption, emission rate and pumping rate are calculated respectively as follows (Desurvire et al., 1990) :

$$W_{12} = \frac{\sigma_{SA}(\lambda_s)\Gamma_s}{h\nu_s A}\left[P_S + P_{ASE}{}^{+} + P_{ASE}{}^{-}\right] \tag{9}$$

$$W_{21} = \frac{\sigma_{SE}(\lambda_s)\Gamma_s}{h\nu_s A}\left[P_S + P_{ASE}{}^{+} + P_{ASE}{}^{-}\right] \tag{10}$$

$$R = \frac{\sigma_{PA}(\lambda_P)\Gamma_P}{h\nu_p A}\left[P_P\right] \tag{11}$$

where σ_{PA} is the ${}^4I_{11/2} \rightarrow {}^4I_{15/2}$ absorption cross sections of the 980 nm forward pumping. σ_{SA} and σ_{SE} are the stimulated absorption and the stimulated emission cross-section of input signal respectively. PASE is the amplified spontaneous emission (ASE) power and A is the effective area of the EDF. The light-wave propagation equations along the erbium-doped fiber can be established as follows (Parekhan et al., 1988):

$$\frac{dP_{ASE}^{\pm}}{dz} = \pm\Gamma(\lambda_{ASE})(\sigma_{se}N_2 - \sigma_{se}N_1)\times P_{ASE}^{\pm} \pm \Gamma(\lambda_s)2h\nu\Delta\nu\sigma_{se}N_2 \mp \alpha P_{ASE}^{\pm} \tag{12}$$

$$\frac{dP_P^{+}}{dz} = \Gamma(\lambda_P)(\sigma_{PE}N_2 - \sigma_{PA}N_1)\times P_P^{+} - \alpha P_P^{+} \tag{13}$$

$$\frac{dP_s^{+}}{dz} = \Gamma(\lambda_s)(\sigma_{se}N_2 - \sigma_{sa}N_1)\times P_s - \alpha P_s \tag{14}$$

Absorption and emission coefficient are essential parameters to know for any types of EDFA modelling. With aid of cutback method the absorption coefficient of fiber was measured experimentally (Hajireza, et al. 2010). For an EDF with uniform radial core doping it is preferred to use the MFD expression developed by (Myslinski et al.,1996). The absorption cross section and emission cross section in room temperature were calculated respectively as follows:

$$\alpha(\lambda) = \sigma\mathrm{a}(\lambda)\Gamma(\lambda)\mathrm{nt} \tag{15}$$

$$\sigma a(\upsilon) = \sigma e(\upsilon)\exp(\frac{h\nu - E_0}{K_B T}) \tag{16}$$

$\sigma_{\mathrm{a}}(\lambda)$ is absorption Cross section that describes the chance of an erbium ion absorbing a photon at wavelength λ. Cross section is given in terms of area because it represents the area is occupied by each erbium ion ready to absorb. Multiplying this by the number of ions, *s*, gives the total area of the fiber cross section that has erbium ready to absorb. The overlapping factors between each radiation and the fiber fundamental mode, Γ (λ) can be expressed as (Desurvire, 1990):

$$\Gamma(\lambda) = 1 - e^{-\frac{2b^2}{\omega_0^2}} \tag{17}$$

$$\omega_0 = a\left(0.761 + \frac{1.237}{V^{1.5}} + \frac{1.429}{V^6}\right) \tag{18}$$

where ω_0 is the mode field radius defined by equation (18), a is the core diameter, b is the Erbium ion-dopant radius and V is the normalized frequency. The absorption and emission cross section has shown in fig.12 (Michael & Digonnet, 1990). Background scattering loss and wavelength-dependent bending loss is represented by α (λ). Wavelength-dependent bending losses used in this numerical model for three different bending diameters as shown in Fig. 13. The bending loss spectral profile is obtained theoretically with help of Marcuse formula (Marcuse, 1982).. These bending radius values are chosen because significant bending losses can be observed in the L-band region. The bending loss profile indicates the total distributed loss for different bending radius associated with macro-bending at different EDF lengths. This information is important when choosing the appropriate bending radius to achieve sufficient suppression of the gain saturation effect in L-band region and reduces the energy transfer from C-band to the longer wavelength region (Giles & Digiovanni, 1990).

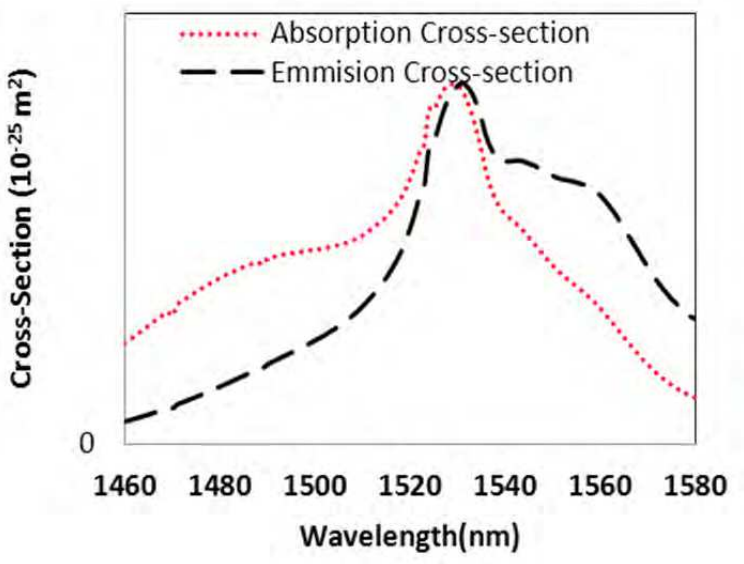

Fig. 12. Absorption and Emission Cross section.

In order to solve the population rate in steady state condition, the time derivatives of for pump and signal powers, equations are set to zero. All the equations are first order differential equations and the Runge-Kutta method is used to solve these equations. The variables used in the numerical calculation and their corresponding values are shown in Table 1.

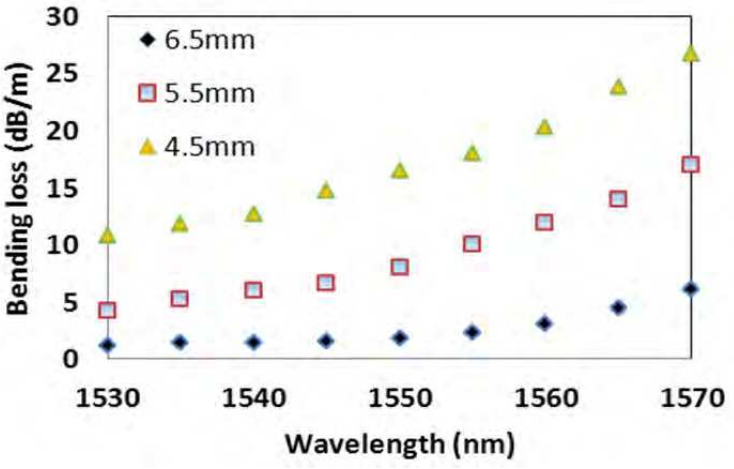

Fig. 13. Bending loss spectral for different bending radius

Parameter	Unit	Value
NA (typ)	0.22	-
λcut-off (typ)	935	[nm]
dcore (typ)	3.3	[μm]
Doping density	1.6	[×1025 ions/m3]
τ (Life time)	10	[ms]
Saturation paramter (typ)	7.985	[×1015 /ms]
λpump	980	[nm]
MFDpump	3.7	[μm]
A	1.633×10^{-11}	m^2
nclad	1.451	-
ncore	1.469	-
λsig	1550	[nm]
MFDsig	5.3	[μm]
Γsig	0.74	-
Γpump	0.77	-
$\sigma_{SA}(\lambda_s)$	2.9105×10^{-25}	m^2
$\sigma_{SE}(\lambda_s)$	4.1188×10^{-25}	m^2
$\sigma_{PA}(\lambda_p)$	2.78×10^{-25}	m^2
$\sigma_{PE}(\lambda_p)$	0.81056×10^{-25}	m^2
Δv	3100	GHz

Table 1. Numerical parameter used in the simulation

The bending loss spectrum of the EDF is measured across the wavelength region from 1530 nm to 1570 nm. Fig. 14 illustrates the bending loss profile at bending radius of 4.5 mm, 5.5 mm and 6.5 mm, which clearly show an exponential relationship between the bending loss and wavelength, with strong dependencies on the fiber bending radius. Bending the EDF causes the guided modes to partially couple into the cladding layer, which in turn results in

losses as earlier reported. The bending loss has a strong spectral variation because of the proportional changes of the mode field diameter with signal wavelength. As shown in Fig. 14, the bending loss dramatically increases at wavelengths above 1550 nm. This result shows that the distributed ASE filtering can be achieved by macro bending the EDF at an optimally chosen radius. It was important to analysis the bending loss in an optimized C-band amplifier before proceed to the next step. The results as shown in Fig. 15 indicate that 3 meter is optimized length for C- band amplifier. It was also seen that with decreasing length, S-band gain is increasing. This happened because of reduction of inversion in C-band region which allow a peak competition for S-band photons to increase. In general C-band always keeps the gain peak unless for longer lengths.

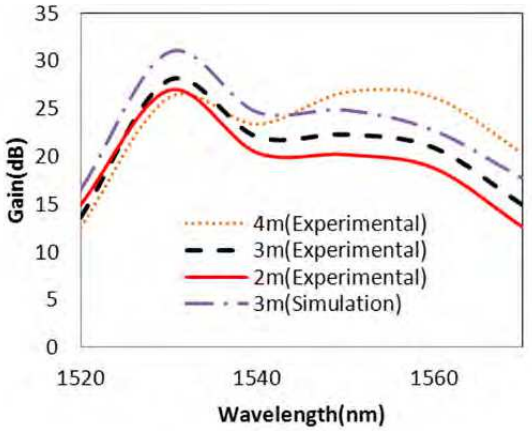

Fig. 14. Different length of unspooled EDFA for -30dBm input signal

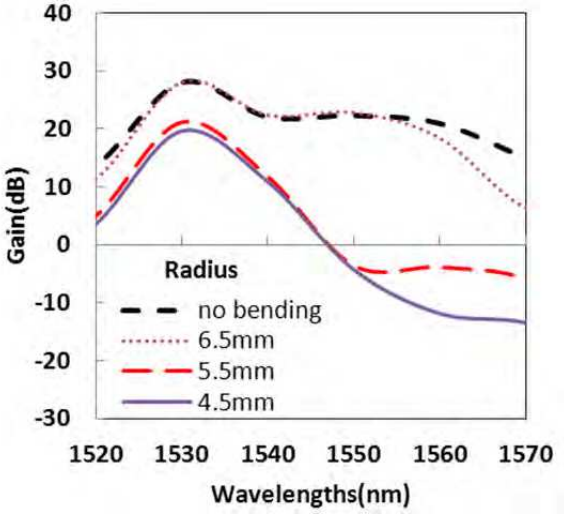

Fig. 15. Efficient length of EDF (3m) in different bending radius for -30dBm input signal (Experimental).

The gain spectrum of the EDFA is then investigated when the optimized length of high concentration EDF spooled in different radius. Fig. 16 shows the gain spectrum of the EDFA with 3m long EDF at different spooling radius. The result was also compared with straight EDF. The input signal power and pump power are fixed at -30dBm and 200 mW respectively in the experiment. As shown in the figure, the original shape of the gain spectrum is maintained in the whole C-band region with the gain decreases exponentially at wavelengths higher than 1560nm. Without bending, the peak gain of 28dB is obtained at 1530 nm which is the reference point to find the optimized length. When the EDF was spooled at a rod with 4.5mm and 5.5mm radius, the shape of gain spectra are totally changed. Finally after trying different radius, 6.5 mm was the optimized radius for this amplifier.

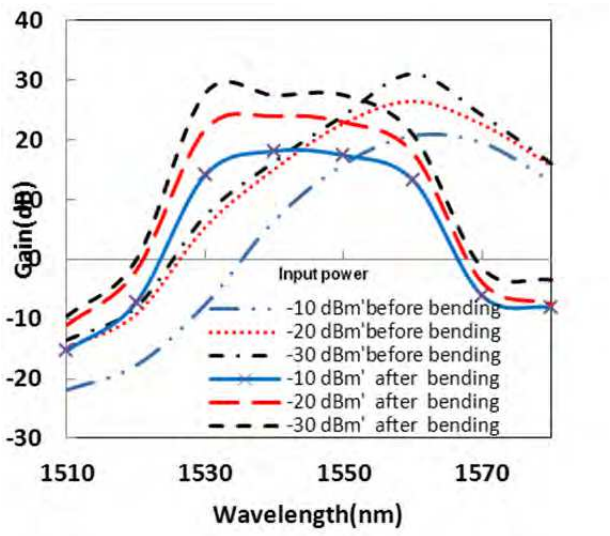

Fig. 16. Gain profile of EDFA with and without macro bending at various input signal power.(Experimental)

As shown in Fig. 14, bending loss at radius of 6.5 mm is low especially at wavelengths shorter than 1560nm and therefore the gain spectrum maintains the original shape of the gain spectrum for un-spooled EDF. To achieve a flatten gain spectrum, the unbent EDFA must operate with insufficient 980nm pump, where the shorter wavelength ASE is absorbed by the un-pumped EDF to emit at the longer wavelength. This will shift the peak gain wavelength from 1530nm to around 1560nm. The macro-bending induces bending loss is dependent on wavelength with an exponential relationship and longer wavelength has a higher loss compared to the shorter wavelength. In relation to the EDFA, the macro-bending also increase the population inversion in C-band due to reduction of gain saturation effect in L-band. Since the L-band gain cannot improve more than a limited value due to exposure bending loss, less C band photons will be absorbed by un-pumped ions to emit at L-band. This effect reduced gain saturation in L-band, so the C-band gain will increase. This increment for peak is not more than the optimized C-band EDFA (3m) since at that level the inversion is in the maximum value. Full inversion for bent EDFA take place at longer length

due to limited energy transfer to longer wavelength. On the other hand, the L-band gain will reduce due to the suppression of L-band stimulated emission induced by macro-bending. The net effect of both phenomena will result in a flattened gain profile.

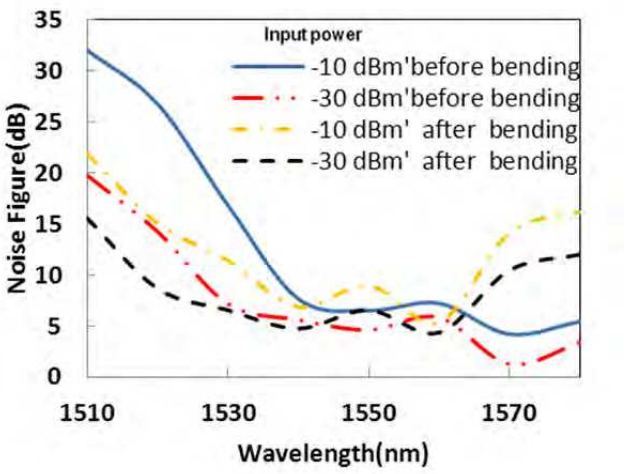

Fig. 17. Noise figure profile of EDFA with and with-out macro bending at various input signal power(Experimental)

Fig. 17 compares the gain spectrum of with and with-out macro bending EDF at various input signal power. The input signal power is varied for -10 dBm to -30 dBm. The input pump power is fixed at 200 mW. The EDF length and bending radius is fixed at 9 meter and 6.5 mm respectively. As shown in the figure, increasing the input signal power decreases the gain but improves the gain flatness. The macro bending also reduces the noise figure of EDFA at wavelength shorter than 1550 as shown in Fig. 18. Since keeping the amount of noise low depends on a high population inversion in the input end of the erbium-doped fiber (EDF), the backward ASE power P –ASE is reduced by the bending loss. Consecutively, the forward ASE power P +ASE can be reduced when the pump power P is large at this part of the EDF which is especially undesirable. This is attributed can be described numerically by the following equation (Harun et al., 2010)

$$NF = \frac{1}{G} + \frac{2P_{ASE}}{Gh\nu} \tag{19}$$

where G is the amplifier's gain, PASE is the ASE power and hv is the photon energy.
Fig 19 indicates the simulation of ASE for standard C-band EDFA (3m) and optimized gain flattened C-band EDFA (9m) after and before bending. ASE here represents population inversion. It clearly explains the gain shifting from longer wavelength to the shorter wavelength due to length increment. Besides effect of bending on gain flattening is explained. Fig 10 is the comparison between standard C-band EDFA with the flattened gain EDFA. We observe a gain variation within ±1 dB over 25 nm bandwidth in C-band region.

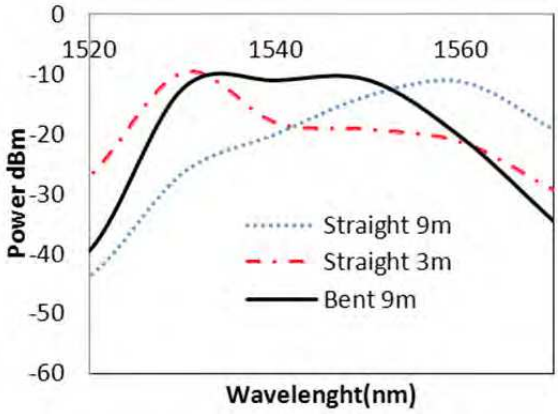

Fig. 18. Amplified Spontaneous emission (Simulation)

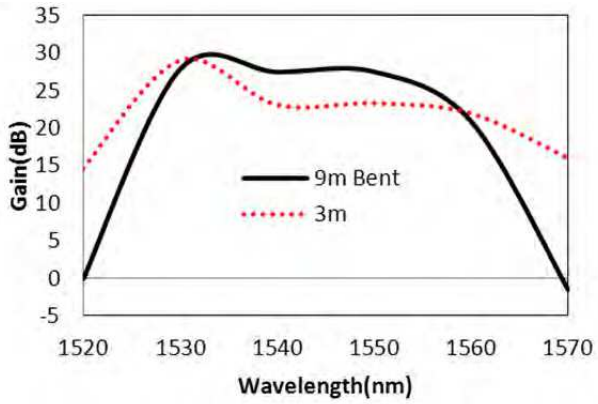

Fig. 19. Comparison of the standard C-band EDFA with the flattened gain EDFA for -30 dB input power(Experimental)

5. Temperature insensitive broad and flat gain EDFA based on macro-bending

Recently, macro-bent EDF is used to achieve amplification in S-band region. In this paper, a gain-flattened C-band EDFA is proposed using a macro-bent EDF. This technique is able to compensate the EDFA gain spectrum to achieve a flat and broad gain characteristic based on distributed filtering using a simple and low cost method. This technique is also capable to compensate the fluctuation in operating temperatures due to proportional temperature sensitivity of absorption cross section and bending loss of the aluminosilicate EDF. This new approach can be used to design a temperature insensitive EDFA for application in a real optical communication (Hajireza, et al. 2010).

The bending loss profile of the erbium-doped fiber (EDF) for various bending radius is firstly investigated by conducting a simple loss- test measurement. In order to isolate the bending loss, the profile is obtained by taking the difference between the loss profile of the same EDF with and without macro-bending across the desired wavelength range. A one meter EDF is used in conjunction with a tunable laser source (TLS) and optical power meter to characterize the bending loss for bending radius of 6.5 mm at wavelength region between 1530 nm and 1570 nm. The bending loss profile indicates the total distributed loss for different bending radius associated with macro-bending at different EDF lengths. This information is important when choosing the optimized bending radius to achieve sufficient suppression of the gain. Fig. 20 illustrates the bending loss profile at bending radius of 6.5 mm at different temperatures, which clearly show an exponential relationship between the bending loss and wavelength. It is also shown that the bending loss in L-band is reduced by increasing the temperature. Bending the EDF causes the guided modes to partially couple into the cladding layer, which in turn results in losses as earlier reported. The bending loss has a strong spectral variation because of the proportional changes of the mode field diameter with signal wavelength. As shown in Fig. 20, the bending loss dramatically increases at wavelengths above 1550 nm. This result shows that the distributed ASE filtering can be achieved by macro bending the EDF at an optimally chosen radius.

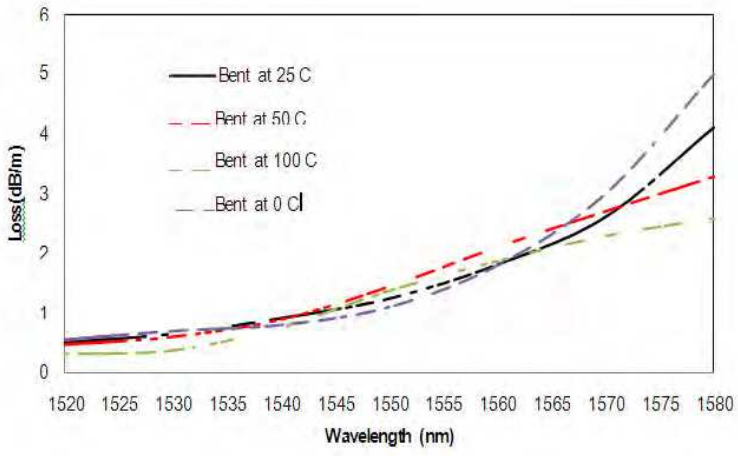

Fig. 20. Loss spectrum of the bent EDF with 6.5 mm bending radius at different temperatures.

Initially, the gain of the single pass EDFA is characterized without any macro-bending at different EDF lengths as shown in Fig. 21. The input signal power is fixed at −30 dBm and the 980 nm pump power is fixed at 200 mW. The wavelength range is chosen between 1520 nm and 1570 nm which cover the entire C-band region. To achieve a flattened gain spectrum, the unbent EDFA must operate with insufficient 980 nm pump, where the shorter wavelength ASE is absorbed by the un- pumped EDF to emit at the longer

wavelength. This will shift the peak gain wavelength from 1530 nm to around 1560 nm. Therefore The EDF length used must be slightly longer than the conventional C- band EDFA to allow an energy transfer from C-band to L-band taking place. This will reduce the gain peak at 1530 nm and increases the gain at longer wavelengths. As shown in Fig. 21, the optimum C-band operation is successfully achieved using only one meter of this high erbium ion concentration EDF. It is also shown that for the lengths longer than 2m gain shifts to longer wavelengths. Figure 22 shows the gain spectrum of the C-band EDFA, which is characterized with macro-bending at different EDF lengths. In the experiment, the input signal power is fixed at -30dBm and the 980nm pump power is fixed at 200mW. These lengths are chosen due to their gain shift characteristics as depicted in Fig. 21. It is important to note that using macro-bending to achieve gain flatness depend on suppression of longer wavelength gains. The macro-bending provides a higher loss at the longer wavelengths and thus flattening the gain spectrum of the proposed C-band EDFA. The combination of appropriate EDF length and bending radius, leads to flat and broad (Hajireza, et al. 2010).

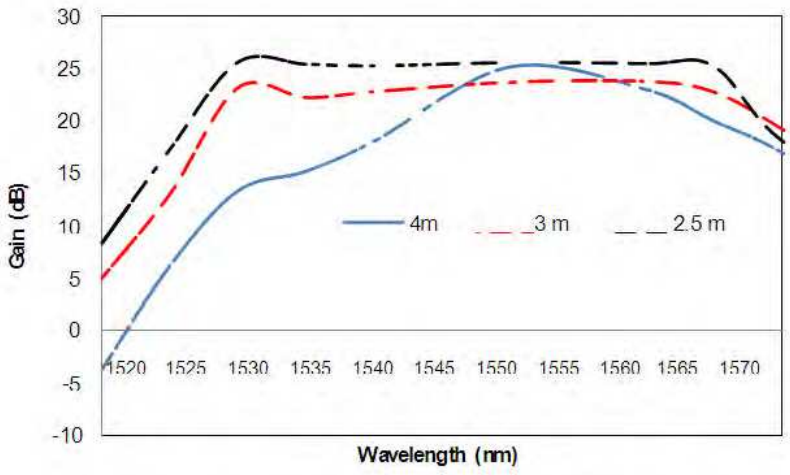

Fig. 21. Gain spectrum of the C-band EDFA

6. Effects of erbium transversal distribution profiles on EDFA performance

Over the past years, Erbium-doped fiber amplifiers (EDFAs) have received great attention due to their characteristics of high gains, bandwidths, low noises and high efficiencies. As a key device, EDFA configures wavelength division multiplexing systems (WDMs) in optical telecommunications, finding a variety of applications in traveling-wave fiber amplifiers, nonlinear optical devices and optical switches. The EDFA uses a fiber whose core is doped with trivalent erbium ions as the gain medium to absorb light at pump wavelengths of 980 nm or 1480 nm and emit at a signal wavelength band around 1500 nm through stimulated

emission. Theoretical study on optimization of rare-earth doped fibers, such as fiber length and pump power has grown along with their increased use and greater demand for more efficient amplifiers (Emamai et al., 2010). Previously, one of the most important issues in improving fiber optic amplifier performance is optimization of the rare-earth dopant distribution profile in the core of the fiber. Earlier approaches to numerical modeling of EDFA performance have assumed that the Erbium Transversal Distributions Profile (TDF) follow a step profile.

Only the portion of the optical mode which overlaps with the erbium ion distribution will stimulate absorption or emission from erbium transitions. The overlap factor equation is defined by (Desurvire, 1982):

$$\Gamma(\lambda) = \frac{2\pi}{N_T} \int_0^{\infty} \Psi(r,\nu) \times n_T(r) \times r \times dr \tag{20}$$

Ψ(r, υ) is the LP01 fiber optic mode envelope, which is almost Gaussian and is defined as :

$$\Psi(r,\nu) = \begin{cases} j_0^2(u_k r/a) & r \le a \\ \dfrac{j_0^2(u_k)}{K_0^2(w_k)} K_0^2(w_k r/a) & r \ge a \end{cases} \tag{21}$$

where J0 and K0 are the respective Bessel and modified Bessel functions and uk and wk are the transverse propagation constants of the LP_{01} mode. N_T is total dopant concentration per unit per length which is defined by:

$$N_T = 2\pi \int_0^{\infty} n_T(r) \times r \times dr \tag{22}$$

Various profiles of erbium transversal distributions can be used for describing mathematical function of EDFA. Two main requirement on choosing erbium transversal distribution functions are; flexibility to be adapted to a collection of profile as broad as possible and dependence on a number of the parameters as low as possible. The optimum transversal distribution function should be (Yun et al., 1999):

$$n_T(r) = n_{T,\max} \exp\{-[|r - \delta| / \theta]^{\beta}\} \tag{23}$$

where nT,maz is the value of the maximum erbium concentration per unit volume. β, θ and δ are distribution profile parameters which construct the profile shapes. θ and β are defined as dopant radius and the roll-off factor of the profile respectively. In practical, it would seem difficult to maintain a high concentration of Erbium in the center of the core, due to diffusion of erbium ions during the fabrication. Modifying the δ value, low ion concentration at the core center can be achieved. The Erbium distribution profiles of EDFA with different values β, θ and δ are depicted in Fig. 22. Figure 22(a) shows several of β values with fixed values of θ=1 and δ=1.5. Figure 22(b) shows the effect of θ values with fix values of δ=1.5 and β=1 while figure 22(c) shows several values of δ changes with fixed values of θ=1 and β =1.5.

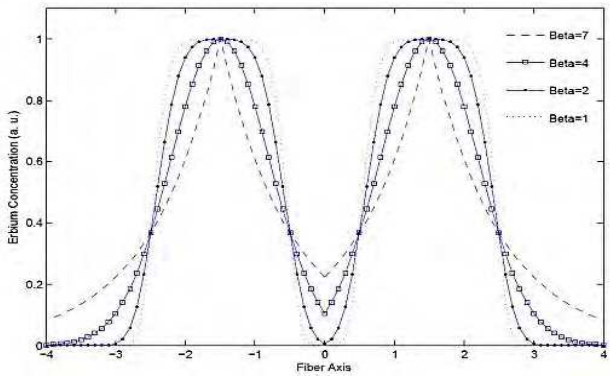

(a)

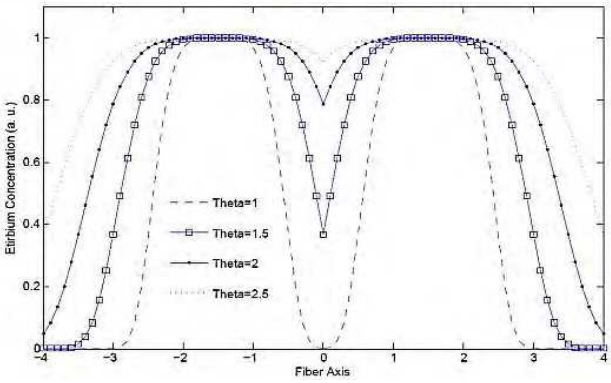

(b)

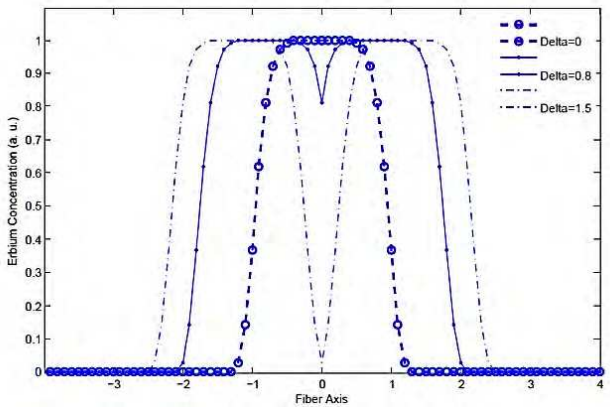

(c)

Fig. 22. The Erbium distribution profile of EDFA (a) at different values of β when, θ=1 and δ=1.5 (b) at different values of θ when δ=1.5 and β=1. (c) at different values of δ when θ=1 and β =1.5.

Figs. 23(a) and (b) demonstrate the gain and noise figure trends of EDFA, respectively at different β and θ values of fiber. The input signal power and input pump power is fixed at -30 dBm and 100 mW respectively while the EDF length is fixed at 14m.

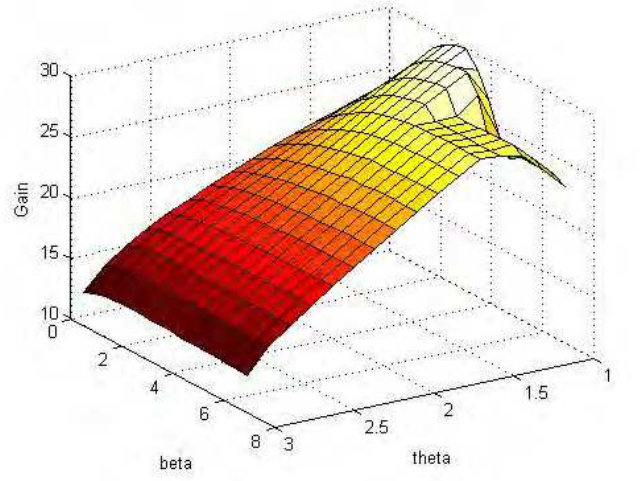

(a)

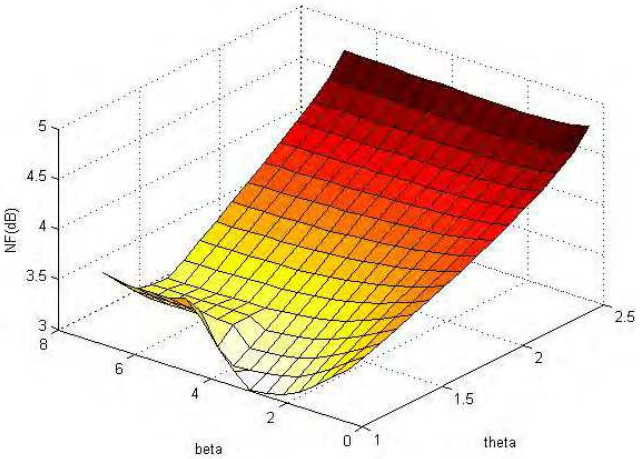

(b)

Fig. 23. (a) Gain profile of EDFA at β=0 (b) Noise figure of EDFA β=0

Fig. 24 shows the gain trends of EDFA at different β and δ values of fiber. The input signal power and input pump power is fixed -30 dBm and 100 mW respectively. The EDF length is 14m long. By comparison between overlap factor and gain results, it is intuitive that the gain result follows the overlap factor values of the fiber. In the low θ values of the fiber in the same EDF concentration the gain decrease by decreasing the θ as depicted on figure 24, this is the results of high erbium intensity at the core and the quenching effect on the fiber amplifier.

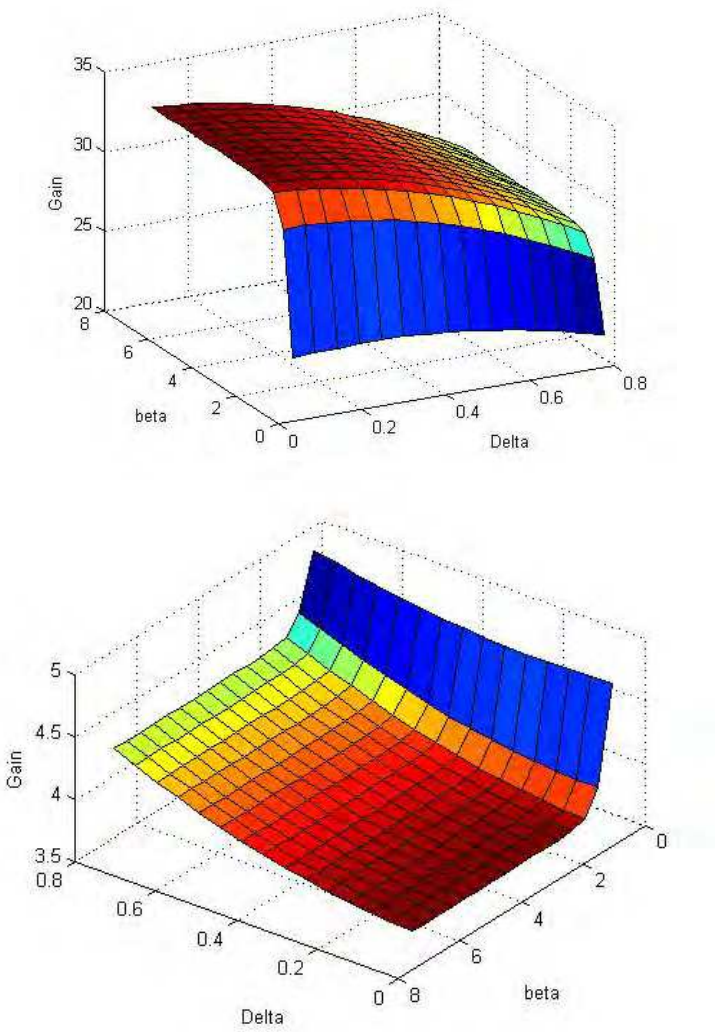

Fig. 24. (a) Gain profile of EDFA at θ=2 (b) Noise figure of EDFA θ=2

The effect of Erbium transversal distribution profile on the performance of an EDFA is investigated. The EDFA uses a 14m long EDF as the gain medium, which is pumped by a 980 nm laser diode via a WDM coupler. An optical isolator is incorporated in both ends of optical amplifier to ensure unidirectional operation. Two types of EDF with the same fiber structure and doping concentration but different on distribution profile are used in the experiment. Fig. 25 shows the Erbium transversal distribution profile of both fibers, which have a doping radius of 2 μm and 4 μm as shown in Figs. 25(a) and (b), respectively. In the experiment, the input signal power and 980nm pump power are fixed at -30dBm and 100 mW respectively.

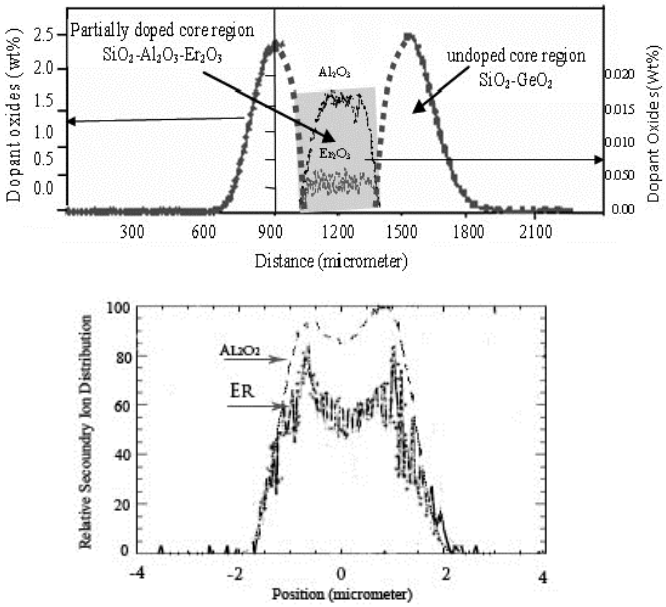

Fig. 25. Erbium TDP. (a) 2μm doping radius (b) 4μm doping

Fig. 26 compares the experimental and numerical results on the gain characteristics for both EDFAs with the 2μm and 4μm doping radius. As expected from the theoretical analysis, the amplifier's gain is higher with 2μm doping radius compared to that of 4μm doping radius at the 1550 nm wavelength region. In the simulation, fiber distribution profile parameters are set as θ=2, β=1.5 and δ=0 for 2μm doping radius which for 4μm doping radius, fiber distribution profile parameters are set as θ=4, β=4 and δ=0.8. The numerical gain is observed to be slightly higher than the experimental one. This is most probably due to splicing or additional loss in the cavity, which reduces the attainable gain. In the case of 4 μm dopant radius, the overlap factor is higher since the overlap happens throughout the core region. However, the high overlap factor will affect the erbium absorption of both the pump and signal. If one considers the near Gaussian profile of the LP01 mode, the erbium in the outer radius of the core tend to be less excited due to the lower pump intensity. The remaining Erbium ions absorption capacity in the outer radius of the core will be channeled to absorbing the signal instead. In the case of 2 μm dopant radius, the overlap factor is lower since the overlap happens only in the central part of the core region. If one considers the near Gaussian profile of the LP01 mode, the erbium in the inner radius of the core tend to be more excited due to the higher pump intensity. Since the outer radius of the core is not doped with Erbium, the lower intensity pump in the outer radius will not be absorbed. The advantage of reduced doping region is that the Erbium absorption only takes place in the central part of the core. Since, the pump intensity is the highest here; the Erbium population can be totally inverted, thus contributing to higher gain. Furthermore, the signal in the outer radius will no longer be absorbed. Hence, the signal will receive a net emission from the erbium which then contributes to higher gain.

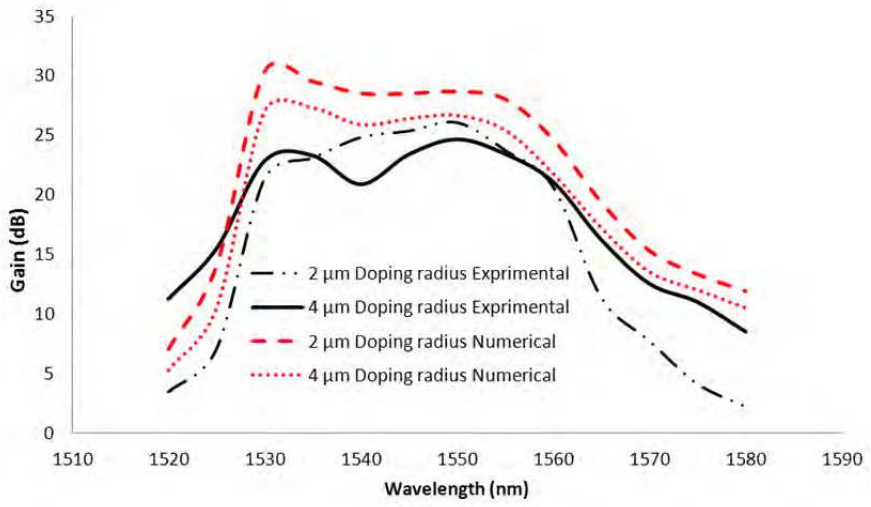

Fig. 26. Numerical and experimental gain comparison of 2µm and 4µm doping radius EDFA

7. Conclusion

In this reserch work a macro-bending approach is demonstrated to increase a gain and noise figure at a shorter wavelength region of EDFA. In the conventional double-pass EDFA configuration , macro-bending improves both gain and noise figure by approximately 6 dB and 3 dB, respectively. These improvements are due to the longer wavelength ASE suppression by the macro-bending effect in the EDF. A new approach is proposed at secound section to achieve flat gain in C-band EDFA with the assistance of macro-bending. The gain flatness is optimum when the bending radius and fiber length are 6.5 mm and 9 meter respectively. This simple approach is able to achieve ±1 dB gain flatness over 25 nm. This cost effective method, which improves the gain variation to gain ratio to 0.1, does not require any additional optical components to flatten the gain, thus reducing the system complexity. The proposed design achieves temperature insensitivity over a range of temperature variation. The gain flatness is optimized when the bending radius and fiber length are 6.5mm and 2.5m respectively. This simple approach is able to achieve 0.5 dB gain flatness over 35nm with no dependency on temperature variations. It is a cost effective method which needs 100mW pump power and does not require any additional optical components to flatten the gain, thus reducing the system complexity. At the end the effect of ETP on the performance of the EDFA is theoretically and experimentally investigated. The ETP can be used to optimize the overlap factor, which affects the absorption and emission dynamics of the EDFA and thus improves the gain and noise figure characteristics of the amplifier. It is experimentally observed that the 1550 nm gain is improved by 3 dB as the doping radius is reduced from 4µm to 2µm. This is attributed to the Erbium absorption

takes place in the central part of the core where the pump intensity is the highest and thus increases the population inversion.

8. References

C.R.Giles, C. A. Burrus, D.Digiovanni, N.K. Dutta and G.Raybon. "Characterization of erbium –doped fibers and application to modeling 980nm and 1480nm pumped amplifiers."IEEE photonics technol. Letter, vol 3, no 4, 363, 1991.

C.R.Giles, D.Digiovanni "spectral dependence of gain and noise in erbium doped fiber amplifier" IEEE photonics technol. Lett., vol. 2, no. 11, 1990

D. Marcuse, "Curvature loss formula for optical fibers," Journal Optical Society America B, vol. 66, pp. 216–220, Mar. 1976.

D. Marcuse, "Influence of curvature on the losses of doubly clad fibers," Applied Optics, vol. 21, pp. 4208–4213, 1982.

D. Marcuse, Light Transmission Optics, 2nd. New York: Van Nostrand Reinhold, , pp. 406–414. ,1982.

E. Desurvire, "Erbium-doped fiber amplifiers: principles and applications", John Wiley & Sons, New York, 1994.

E. Desurvire, J. L. Zyskind, C. R. Giles, "Design Optimization for Efficient Erbium-Doped Fiber Amplifiers" Journal of Lightwave Technology, vol. 8. no. 11, November 1990.

G.P. Agrawal, Fiber-Optic Communication Systems, 2nd ed. Wiley, New York, NY, 1997.

Gred, Keiser. Optical Fiber Communications. Singapore: McGraw-Hill, 2000.

Hassani, E. Arzi, F . Seraji "Intensity based erbium distribution for erbium doped fiber amplifiers" Optic Quantum Electron, vol. 39, no. 1, pp: 35-50, 2007.

J. C. Martin"Erbium transversal distribution influence on the effectiveness of a doped fiber: optimization of its performance on the effectiveness of a doped fiber: optimization of its performance" vol. 194, pp. 331-339, 2001

J. Michael, F. Digonnet, "Rare-earth-doped Fiber Lasers and Amplifiers" CRC Press,

J. R. Armitage "Three-level fiber laser amplifier: a theoretical model", APPLIED OPTICS, Vol. 27, no. 23, 1988

K. Thyagarajan and C. Kakkar, "S-Band Single-Stage EDFA With 25-dB Gain Using Distributed ASE Suppression", IEEE Photonics Technol. Lett. 16 (11), (2004).

P. F. Wysocki, R. E. Tench, M. Andrejco, and D. DiGiovanni, in Proceedings of Optical Fiber Communications, OFC'97, pp. 127-129 Dallas, TX,1997.

P. F. Wysocky, in Proceedings of Optical Fiber Communications, OFC'98, pp. 97-99, San Jose, CA,1998.

P. Hajireza , S. D. Emami, C. L. Cham, D. Kumar, S. W. Harun and H. A. Abdul-Rashid" Linear All-fiber Temperature Sensor based on Macro-Bent Erbium Doped Fiber" ,Laser Physycs Letter, vol. 7, No. 10, pp. 739-742, 2010

P. Hajireza , S. D. Emami, S. Abbasizargaleh, S. W. Harun and H. A. Abdul-Rashid "Optimization of Gain flattened C-band EDFA using macro-bending" Laser Physics Letter, Vol. 20, No. 6, pp. 1–5 , 2010

P. Hajireza, S. D. Emami, S. Abbasizargaleh, S. W. Harun, D. Kumar and H. A. Abdul-Rashid, „Application of Macro-Bending for Flat and Broad Gain EDFA“ Journal of Modern Optics, 2010

P. Hajireza, S. D. Emami, S. Abbasizargaleh, S. W. Harun, D. Kumar, and H. A. Abdul-Rashid "Temperature Insensitive Broad And Flat Gain C-Band Edfa Based On Macro-Bending", Amplifier" Progress In Electromagnetics Research C, Vol. 15, Pp. 37-48

P. Myslinski and J. Chrostowski, "Gaussian mode radius polynomials for modeling doped fiber amplifiers and lasers," Microwave OpticTechnology Letter, vol. 11 no. 2, pp. 61–64, 1996.

Parekhan M. Aljaff, and Banaz O. Rasheed "Design Optimization for Efficient Erbium-Doped Fiber Amplifiers" World Academy of Science, Engineering and Technology, 2008

S. A. Daud, S. D. Emami, K. S. Mohamed, H. A. Abdul-Rashid, S. W. Harun, H. Ahmad, M. R. Mokhtar, Z. Yusoff' and F. A. Rahman, in Proceedings of IEEE Conference on Photonics Global Institute of Electrical and Electronics Engineers, Singapore, pp. 1-3, 2008.

S. A. Daud, S. D. Emami, K. S. Mohamed, N. M. Yusoff, L. Aminudin, H. A. Abdul-Rashid, S. W. Harun, H. Ahmad, M. R. Mokhtar, Z. Yusoff and F. A. Rahman, "Gain and Noise Figure Improvements In a Shorter Wavelength Region of EDFA Using A Macro-Bending Approach", vol.18, no. 11, pp. 1362-1364, 2008.

S. D. Emami, P. Hajireza, F. Abd-RahmanF. Abd-Rahman, H. Ahmad, "wide-band hybrid amplifier operating in s-band region" Progress In Electromagnetics Research, PIER pp. 301, 313, 2010.

S. D. Emami, S. W. Harun, F. Abd-Rahman, H. A. Abdul-Rashid, S. A. Daud, and H. Ahmad "Optimization of the 1050nm Pump Power and Fiber Length in Single-pass and Double-pass Thulium Doped Fiber Amplifier" PIERB 14 , pp. 431-448, 2009.

S. W. Harun, K. Dimyati, K. K. Jayapalan, and H. Ahmad, "An Overview on S-Band Erbium-Doped Fiber Amplifier," Laser Physics Letter, vol. 4 , pp. 10–15, 2006.

S.K. Yun et al., Dynamic erbium-doped fibre amplifier based on active gain flattening with fibre acoustooptic tunable filter, IEEE Photonics Technology Letter. Vol. 11 pp. 1229–1231,1999.

S.W. Harun, , S.D. Emami, F. Abd Rahman, S.Z. Muhd-Yassin, M.K. Abd-Rahman, and H. Ahmad "Multiwavelength Brillouin/Erbium Ytterbium fiber laser" Laser Physiccs Journal, pp: 1-3,2007

S.W. Harun, R. Parvizi, X.S. Cheng, A. Parvizi, S.D. Emami, H. Arof and H. Ahmad ' Experimental and theoretical studies on a double-pass C-band bismuth-based erbium-doped fiber amplifier 'Optics & Laser Technology, vol. 42, no. 5, pp. 790-793 , July 2010

T. Pfeiffer, H. Bulow "Analytical Gain Equation for Erbium-Doped Fiber Amplifiers Including Mode Field Profiles and Dopant Distribution" IEEE Photonics Technology Letters, vol. 4, no. 5 , May 1992

Uh-Chan Ryu, K. Oh, W. Shin, U. C. Paek, IEEE Journal of Quantum Electronic vol. 38, pp. 149-161, 2002.

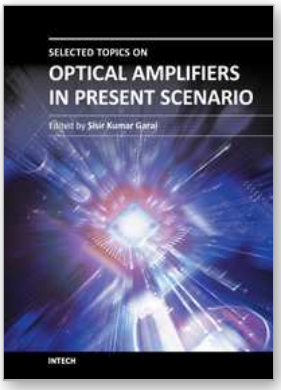

Selected Topics on Optical Amplifiers in Present Scenario

Edited by Dr. Sisir Garai

ISBN 978-953-51-0391-2
Hard cover, 176 pages
Publisher InTech
Published online 23, March, 2012
Published in print edition March, 2012

With the explosion of information traffic, the role of optics becomes very significant to fulfill the demand of super fast computing and data processing and the role of optical amplifier is indispensable in optical communication field. This book covers different advance functionalities of optical amplifiers and their emerging applications such as the role of SOA in the next generation of optical access network, high speed switches, frequency encoded all-optical logic processors, optical packet switching architectures, microwave photonic system, etc. Technology of improving the gain and noise figure of EDFA and, the study of the variation of material gain of QD structure are also included. All the selected topics are very interesting, well organized and hope it will be of great value to the postgraduate students, academics and anyone seeking to understand the trends of optical amplifiers in present scenario.

How to reference

In order to correctly reference this scholarly work, feel free to copy and paste the following:

Siamak Emami, Hairul Azhar Abdul Rashid, Seyed Edris Mirnia, Arman Zarei, Sulaiman Wadi Harun and Harith Ahmad (2012). Doped Fiber Amplifier Characteristic Under Internal and External Perturbation, Selected Topics on Optical Amplifiers in Present Scenario, Dr. Sisir Garai (Ed.), ISBN: 978-953-51-0391-2, InTech, Available from: http://www.intechopen.com/books/selected-topics-on-optical-amplifiers-in-present-scenario/doped-fiber-amplifier-characteristic-under-internal-and-external-perturbation

INTECH
open science | open minds

InTech Europe
University Campus STeP Ri
Slavka Krautzeka 83/A
51000 Rijeka, Croatia
Phone: +385 (51) 770 447
Fax: +385 (51) 686 166
www.intechopen.com

InTech China
Unit 405, Office Block, Hotel Equatorial Shanghai
No.65, Yan An Road (West), Shanghai, 200040, China
中国上海市延安西路65号上海国际贵都大饭店办公楼405单元
Phone: +86-21-62489820
Fax: +86-21-62489821